Image States: Binding Energies, Effective Masses, and Surface Corrugation

N. Garcia, B. Reihl, K. H. Frank, and A. R. Williams
IBM Zurich Research Laboratory, 8803 Rüschlikon, Switzerland
(Received 5 September 1984)

We show that image-potential surface states are strongly affected by surface corrugation. In particular, their binding energy and effective mass are strongly coupled. New inverse-photoemission measurements for Ag(100) indicate that neglect of the corrugation contribution to the binding in previous work has caused (i) the confusion of the fundamental and excited image states and (ii) underestimation, by a factor of 3, of the spatial extent of the states observed.

PACS numbers: 73.20.Cw, 79.20.Kz, 79.60.Cn

We are concerned here with a special class of unoccupied electronic states that exist at solid surfaces. The potential that binds an electron to the surface in such a state is due to the response of the surface to the presence of the electron, i.e., the electron is bound to its own image.[1,2] We want to emphasize that the physical origin of image states, which have now been observed on several metal surfaces by LEED[3,4] and by inverse photoemission,[5-8] differs qualitatively from that of Shockley states[9] which are created at surfaces by the breaking of crystalline interatomic bonds. Unlike image states, the latter are part of the manifold of atomic valence states, and emerge, e.g., in a tight-binding description of a surface.[10] Unoccupied Shockley states have also been observed by inverse photoemission.[11]

Image states are bound weakly to the surface, implying that their amplitude is concentrated relatively far away from it.[2,4] The physical picture of these states that we present is similar to that for electrons at semiconductor inversion layers, i.e., the electron is localized in one direction (z), but is nearly free in the remaining two directions (x and y). In the case of image states, because the localization is provided by a Coulomb potential, the z dependence of the wave function is fundamentally hydrogenic, with the crystal surface playing a role analogous to that of the atomic core in an alkali-metal atom (i.e., quantum defect). Interaction with the surface also perturbs the x,y dependence of the image-state wave function, causing motion along the surface to depart somewhat from free-electron behavior. This departure is measured directly in inverse-photoemission experiments as the effective mass.[6,8] An important aspect of the present work is the observation that *comcomitant with any deviation of the effective mass m_n^* from unity is an increase of the image-state binding energy E_B.*

That the binding energy and the effective mass are linked follows from general theoretical considerations, but determination of the magnitude of the effect requires either a detailed electronic-structure calculation for the surface, or accurate measurements of both the binding energy and the effective mass. Our measurements of these quantities for the (100) surface of Ag, shown in Fig. 1, indicate that, even on such dense surfaces, the surface-corrugation effect is not merely nonnegligible; it provides two-thirds of the image-state binding energy, and has caused the misidentification of image states previously observed on the (100) surface of Cu[6,7] and Au.[7] These states were ascribed to

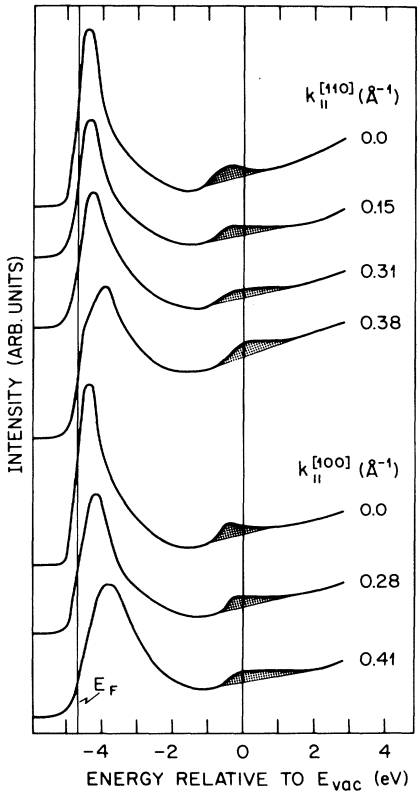

FIG. 1. Inverse-photoemission data taken at $h\nu = 9.7$ eV for Ag(100) showing structure due to image states ~ -0.6 eV below vacuum. Data taken for several angles of electron incidence permit a lower bound to be placed on the effective mass for motion of the image electron along the corrugated surface ($m^* \geq 1.3m$) in both azimuths. Also note the increasing width of the image-state feature (shaded) with increasing $k_{\parallel}$. The emission feature near E_F is mainly bulk derived (Refs. 5, 6, and 8). For details of the experiment see Refs. 8 and 11.

the nodeless fundamental hydrogenic state ($n=1$ in Fig. 2), whereas the present analysis shows that the states observed on these surfaces at about -0.6 eV below the vacuum level E_{vac} are, in fact, the first excited image state ($n=2$ in Fig. 2), possessing a node at ~ 5 Å from the surface and a maximum at ~ 12 Å (see Fig. 2). Note that the importance of surface corrugation to the binding energy implies that the binding energy observed experimentally does not directly indicate the spatial extent of the image state. The latter is determined exclusively by the hydrogenic component of the binding energy ϵ_n. This distinction is particularly important in the present context, because the spatial extent of the states of a Coulomb potential varies more strongly with energy than those of short-range potentials.

The fundamental physical parameters characterizing the problem; the geometry, length, and energy scales, are shown in Fig. 2. Note that most of the amplitude of the states with which we are concerned is concentrated at distances from the surface greater than those characteristic of atomic valence states. It is not surprising, therefore, that the z dependence of the wave function is fundamentally that of a planar hydrogenic atom. As Fig. 2 also indicates, for their existence these states require a gap 2Δ which serves as the repulsive barrier that prevents the electron and its image from combining to form a neutral bulk quasiparticle.

In a one-dimensional model[12,13] containing the essential aspects of these quantum-defect surface states, a gap in the otherwise free-electron spectrum of the substrate is created by a single nonzero pseudopotential coefficient. (The position of this gap is fixed by the work-function and self-consistent band-structure calculations.[12]) The distance relative to the image plane at which the single-particle potential becomes imagelike is given by z_0 (see Fig. 2).[14] This model is solved here analytically to obtain states such as those shown in Fig. 2. The model confirms our intuitive expectation that excited ($n \geq 2$) image states are very insensitive to the parameters characterizing the substrate, the bandwidth, the band gap, and z_0, because the wave-function maximum is farther away from the surface (cf. Fig. 2). This does not hold for the fundamental $n=1$ state.

Consider now the transverse (x,y) variation of the wave function of such states. As stated, this aspect of the problem should be an excellent candidate for nearly-free-electron theory. If the surface is dense, the corrugation will be small and the smallest surface reciprocal-lattice vector $G(1,0)=2\pi/a_s$ (a_s is the surface lattice constant) is large. Under these conditions, we expect deviations from free-electron behavior to be characterized by a single matrix element $V_n(1,0)$ of the effective single-particle potential, and perturbation theory to be adequate ($V_n < \hbar^2 G^2/m$). In what follows, we take this corrugation matrix element to be a parameter.[15] Both the rigid displacement of the free-electron parabolic dispersion curve E^n_{corr} (the contribu-

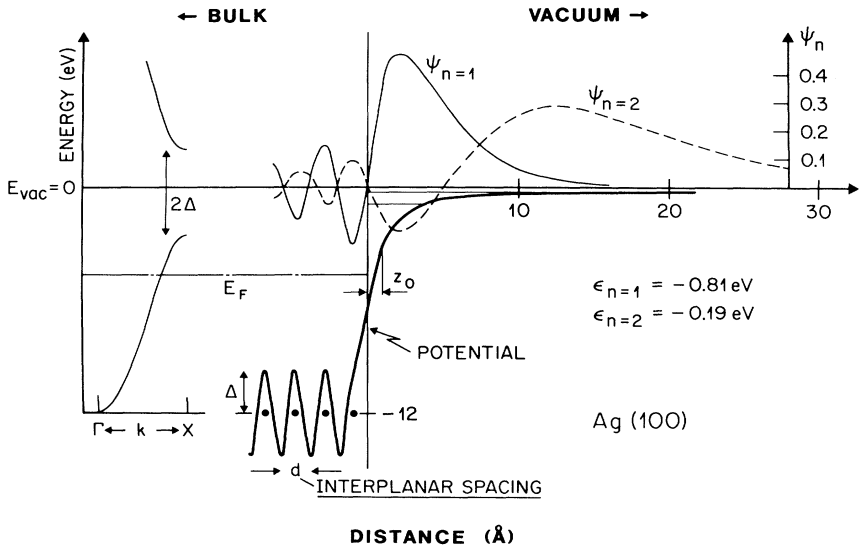

FIG. 2. Energy and spatial scales characterizing image states on metal surfaces. Shown are the fundamental ($n=1$) image state, with no nodes in the vacuum region, and the first excited ($n=2$) image state, with one node. Also shown are the effective one-electron potential and the bulk energy-band structure that produce these image states. The quantity z_0 (taken to be ~ 1 Å) specifies the distance from the surface beyond which the potential is purely Coulombic (imagelike). The parameters Δ, width of the gap, its position, and the Fermi energy E_F have been taken from self-consistent band-structure calculations (Ref. 12). The image plane corresponds to $z=0$.

tion of corrugation to the binding energy) and its deviation from perfect parabolicity (the deviation of the effective mass from unity) are determined in second-order perturbation theory directly by the single corrugation parameter; the formulas are

$$E_B^n = \epsilon_n + E_{\text{corr}}^n + \hbar^2 k_{\parallel}^2 / 2m_n^*, \quad (1)$$

with

$$E_{\text{corr}}^n = 8m|V_n|^2/\hbar^2 G^2, \quad (2)$$

$$m_n^*/m = (1 - 128m^2|V_n|^2/\hbar^4 G^4)^{-1}. \quad (3)$$

Figure 3 shows how the theoretical link between the binding energy and the effective mass [Eqs. (1)–(3)] relates to available experimental data.[6–8] In particular, Fig. 3 shows the importance of the lower bound obtained in the present measurements of the effective mass to the question of the magnitude of surface-corrugation effects. In our view, the fact that the effective mass for the image state on Ag(100) is at least 30% greater than unity can be reconciled with a binding energy near −0.6 eV only if the state is taken to be the first excited image state (see Fig. 2), whose hydrogenic binding energy $\epsilon_{n=2}$ is only about −0.2 eV.

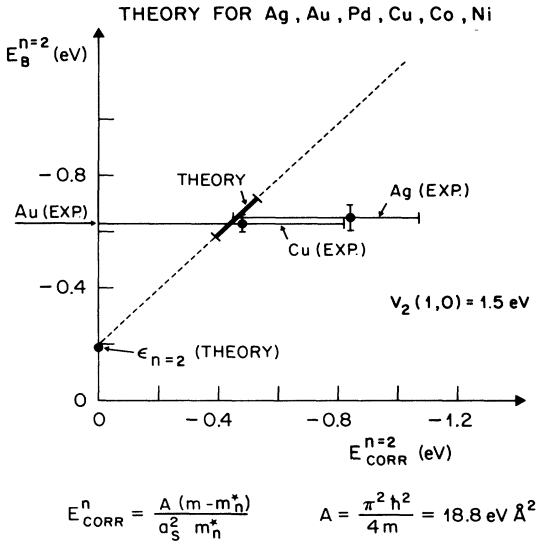

FIG. 3. Relationship between total image-state binding energy and the effective mass. The lower bound of 1.3 for the effective mass on Ag(100) obtained in the present experiments, together with the binding energy of −0.6 eV observed, shows that two-thirds of the total binding energy is due to the corrugation contribution. The state considered is the first excited image state. The corrugation matrix element and the hydrogenic component of the binding energy (−0.2 eV) deduced from the measurements on Ag(100) permit the total binding energy and effective mass to be predicted for the corresponding image state on other dense metal surfaces.

Note that, since the hydrogenic component of the binding energy must be negative, the theory places an *upper* bound on the effective mass of 1.5. (The theoretical upper bound on the effective mass, for any binding energy, corresponds in Fig. 3 to 45° line passing through the origin.) Since the spatial extent of the image state increases rapidly as the hydrogenic component of the binding energy decreases, an effective mass m_2^* near the experimental lower limit of 1.3 and a hydrogenic binding energy near −0.2 eV constitute the most plausible interpretation of the data. Note that the value of 1.2 estimated for the effective mass for Cu(100) in Ref. 6 equals our predicted value.

Several independent factors support this interpretation: First, not only are our data for Ag(100) naturally explained, but also the previously measured binding energies for image states on Au(100) and Cu(100) (see Fig. 3), with the similarity of the three binding energies stemming from a weak dependence of the hydrogenic component of the binding energy on surface properties (for the excited image state). Note that the range of reasonable effective masses leads to only a narrow range of total binding energies. Second, interpreting the state at −0.6 eV as an excited state leaves the fundamental image state to possibly contribute to the surface sensitivity observed for the mainly bulk-derived emission feature near the Fermi level (~ -4 eV) in Fig. 1. We observe that both the −0.6-eV and the Fermi-level peaks diminish rapidly with small amounts of adsorbed water; this has also been observed for Cu(100) with Cl adsorption.[6] Third, if we ascribe image-state feature in Fig. 1 to the superposition of all $n \geq 2$ hydrogenic states, the increasing width of the feature with $k_{\parallel}$ is naturally explained, since the more excited states $n \geq 3$ will have less perturbed masses ($m_n^* \rightarrow m$). Finally, a single reasonable value of the only significant parameter of our model, $V_n(1,0)$, accounts for all existing data (Cu,Ag,Au) and predicts that the binding energy and effective mass for Ni(100) are the same as those of Cu(100), since their lattice constants are similar.

We thank A. Baratoff for discussions, and R. Schlittler for technical assistance.

[1]M. W. Cole and M. H. Cohen, Phys. Rev. Lett. **23**, 1238 (1969).

[2]N. Garcia and J. Solana, Surf. Sci. **36**, 262 (1973).

[3]E. G. McRae and C. W. Caldwell, Surf. Sci. **7**, 41 (1967); for a review of these resonances in LEED, see E. G. McRae, Rev. Mod. Phys. **51**, 541 (1979).

[4]P. M. Echenique and J.B. Pendry, J. Phys. C **11**, 2065 (1978).

[5]P. D. Johnson and N. V. Smith, Phys. Rev. B **27**, 2527 (1983).

[6]V. Dose, W. Altmann, A. Goldmann, U. Kolac, and

J. Rogozik, Phys. Rev. Lett. **52**, 1919 (1984).

[7]D. Straub and F. J. Himpsel, Phys. Rev. Lett. **52**, 1922 (1984).

[8]B. Reihl, K. H. Frank, and R. R. Schlittler, Phys. Rev. B **30**, 7328 (1984).

[9]W. Shockley, Phys. Rev. **56**, 317 (1939).

[10]K. M. Ho, B. N. Harmon, and S. H. Liu, Phys. Rev. Lett. **44**, 1531 (1980).

[11]B. Reihl, R. R. Schlittler, and H. Neff, Phys. Rev. Lett. **52**, 1826 (1984).

[12]H. Eckardt, L. Fritsche, and J. Noffke, J. Phys. F **14**, 97 (1984); F. M. Mueller, A. J. Freeman, J. O. Dimmok, and A. M. Furdyna, Phys. Rev. B **1**, 4167 (1970); V. L. Moruzzi, J. F. Janak, and A. R. Williams, *Calculated Electron Properties of Metals* (Pergamon, New York, 1969); F. J. Himpsel and D. E. Eastman, Phys. Rev. B **21**, 3207 (1980).

[13]N. Garcia, J. Solana, and N. Carbrera, Surf. Sci. **38**, 455 (1973), following the perturbative approach for atom-surface scattering of N. Carbrera, V. Celli, F. O. Goodman, and J. R. Manson, Surf. Sci. **19**, 67 (1970).

[14]The effective single-particle potential is interpolated linearly in the region between the outermost atomic plane and the z_0 value at which the potential becomes imagelike. The slope of the linear portion of the potential is very similar to the slope of the local-density potential for the self-consistent jellium surface.

[15]$V_n(1,0)$ is taken to be proportional to $|\psi_n|^2$ at its innermost maximum (~ 2 Å in Fig. 2). The proportionality factor is the single parameter, which we deduce from the experimentally accessible $n=2$ state.